ELSEVIER

Applied Catalysis A: General 193 (2000) 71–86

APPLIED
CATALYSIS
A: GENERAL

www.elsevier.com/locate/apcata

Activity, selectivity and stability of Ni and bimetallic Ni–Pt supported on zeolite Y catalysts for hydrogenation of acetophenone and its substituted derivatives

R.V. Malyala[b], C.V. Rode[a], M. Arai[c], S.G. Hegde[a], R.V. Chaudhari[a,*]

[a] Homogeneous Catalysis Division, National Chemical Laboratory, Pune 411 008, India
[b] CANMET Energy Technology Centre, Natural Resources Canada, 1 Haanel Drive, Nepean, Ont., Canada K1A 1M1
[c] Institute for Chemical Reaction Science, Tohoku University, Katahira, Aoba-ku, Sendai, 980, Japan

Abstract

The hydrogenation of acetophenone, p-hydroxy acetophenone (p-HAP) and p-isobutyl acetophenone was studied using Ni and bimetallic Ni–Pt supported on zeolite Y catalysts. A 10% Ni-supported-on-zeolite Y catalyst showed the optimum activity when compared to other Ni-supported catalysts. The activity of this catalyst decreased very rapidly on recycle; however, the bimetallic Ni–Pt-supported-on-zeolite Y catalyst was highly stable and showed constant activity on recycle. The addition of Pt catalyses the reduction of Ni^{2+} to Ni^0, as characterised by X-ray photoelectron spectroscopy (XPS) and other techniques. For the Ni–Pt bimetallic catalyst, the hydrogen adsorption was found to be higher than that for monometallic catalysts; the adsorbed hydrogen reacts with the activated acetophenone complex to facilitate the catalytic process. The FTIR analysis of adsorbed acetophenone on the catalyst samples indicated that, in both monometallic and bimetallic catalysts supported on zeolite Y, the C=O bond of acetophenone is highly activated due to the strong interactions with the acidic sites present on the zeolite. Zeolite interactions with intermediate products and solvent moieties also influenced the selectivity behaviour. A trace amount of a base like NaOH acts as a promoter in improving the selectivity towards alcohol. A plausible reaction mechanism has been proposed for the hydrogenation of acetophenone and its derivatives using monometallic as well as bimetallic catalysts. ©2000 Elsevier Science B.V. All rights reserved.

Keywords: Catalytic hydrogenation; Acetophenone and derivatives; Nickel catalysts; Bimetallic catalysts

1. Introduction

Catalytic hydrogenation of organic compounds containing carbonyl groups is important in a variety of chemical processes for the synthesis of fine chemicals and pharmaceuticals [1]. Some important

* Corresponding author. Tel.: +91-20-5893260; fax: +91-20-5893260.
E-mail address: rvc@ems.ncl.res.in (R.V. Chaudhari).

examples of this category are the hydrogenation of 1-phenyl ethanone (acetophenone) and its substituted derivatives such as 1-(4-hydroxy phenyl) ethanone (p-hydroxy acetophenone) and 1-(4-isobutylphenyl) ethanone (p-isobutyl acetophenone) to their corresponding secondary alcohols. These reactions are usually carried out in liquid phase using supported metal catalysts. The selective hydrogenation of p-isobutyl acetophenone to 1-(4-hydroxyphenyl) ethanol (p-isobutyl phenyl ethanol (p-IBPE)) is

important in the synthesis of Ibuprofen, a non-steroidal anti-inflammatory drug. This new catalytic route proposed by Hoechst–Celanese and Boots is considered as a major innovation from economic as well as environmental viewpoints [2,3]. Since many side products are formed during the course of hydrogenation in such complex multistep reactions, the selectivity to a desired product is an important issue. In several reports, supported metal catalysts consisting of Ni, Pt, Pd and Rh have been suggested for the hydrogenation of acetophenone, but for the hydrogenation of p-hydroxy acetophenone and p-isobutyl acetophenone, most of the literature is patented and there are only a few reports which deal with the catalytic aspects involved in such important reactions [2–6]. It is well known that supported bimetallic catalysts can be advantageous over the monometallic systems to achieve higher activity, stability and in some cases, higher selectivity [7,8]. These aspects have not been investigated in detail for the hydrogenation of acetophenone and its derivatives, except the work of Masson et al. [9], Hammar-Thibault et al. [10], and more recently, the work of Rajashekharam and Chaudhari [11], using the Ni–Pt bimetallic catalyst system for the hydrogenation of acetophenone and its derivatives.

The aim of this work was to study the hydrogenation of acetophenone and its derivatives using monometallic Ni-supported and bimetallic Ni–Pt-supported-on-zeolite Y catalysts and an attempt has been made to correlate the structure-activity and structure-stability behaviour of various catalysts. For this purpose, the catalysts were characterised using different techniques such as X-ray diffraction (XRD), temperature programmed desorption (TPD) of H_2, temperature programmed reduction (TPR), transmission electron microscopy (TEM), X-ray photoelectron spectroscopy (XPS) and in situ FTIR. A suitable reaction mechanism for the hydrogenation of acetophenone has also been proposed.

2. Experimental

2.1. Catalyst preparation

Monometallic Ni-supported-on-zeolite Y catalysts (Ni content in % w/w) were prepared by a precipitation technique following the procedure described earlier [12]. For this purpose, the support zeolite Y (Si/Al = 4.5) was calcined for 4 h before use at 773 K. A slurry of the support was made in distilled water and stirred for 2 h at 363 K. To this hot solution, a known amount of Ni $(NO_3)_2 \cdot 6H_2O$ was added. After stirring for 6 h, 10% ammonium carbonate solution was added dropwise. The addition continued till a pH value of 10 was attained. The resulting slurry was filtered to obtain a green cake and a colourless filtrate, confirming the complete precipitation of Ni as Ni carbonate. The AAS analysis revealed the absence of Ni in the filtrate. The cake was dried overnight at 383 K and was calcined in a static air furnace at 773 K for 10 h. The reduction of the catalyst was carried out at 773 K at an H_2 flow rate of $5 \times 10^{-5} m^3 min^{-1}$ for 10 h.

Bimetallic Ni–Pt catalyst was prepared by charging the Ni-supported-on-zeolite Y catalyst before calcination to a toluene solution containing Pt (C_8H_{12}) Cl_2 as Pt precursor. This suspension was refluxed for 4 h and the excess toluene was removed using a rotavapor. The powder obtained was calcined and reduced in the same manner as described above. Thus, a series of catalysts with varying Pt contents (in % w/w) were prepared by this method. The detailed specifications of these catalysts are Ni content: 5–20% (w/w), Pt content: 0–2% (w/w), particle size: $1 \times 10^{-5} m$, surface area of support: $5 \times 10^5 m^2 kg^{-1}$, particle density: $2.5 \times 10^3 kg m^{-3}$, pore volume: $3 \times 10^{-4} m^3 kg^{-1}$, porosity: 0.58.

2.2. Catalyst characterisation

XRD analysis of the catalyst samples were carried out by Phillips model no. 1730 using Ni filtered Cu Kα radiation and a proportional counter detector at a scan rate of $4° min^{-1}$. The average crystallite size of metallic Ni was calculated using the Scherrer equation [13,14].

TPD and TPR experiments were carried out in a similar apparatus described elsewhere [15,16]. For TPD, a sample of $7.5 \times 10^{-5} kg$ was reduced under H_2 flow at 673 K for 1 h and cooled to room temperature. The sample was heated in flowing argon up to adsorption temperature from 303 to 573 K. After the sample reached the desired temperature, argon was switched to hydrogen flowing at $5 \times 10^{-5} m^3 min^{-1}$; the temperature was maintained for 4 min, after which

the sample was cooled to 303 K. The sample was then heated at a rate of 30 K min^{-1} up to 723 K and at an argon flow rate of 3×10^{-5} m^3 min^{-1}. The TPD of H$_2$ was monitored by a thermal conductivity detector (TCD). The TPD was repeated a few times for the same sample in order to obtain reproducible spectra. For TPR, a gas stream of 10% hydrogen in argon was passed through the sample (7.5×10^{-5} kg) in a quartz reactor heated at 10 K min^{-1} up to 1023 K with a temperature-programmed furnace. The water produced by reduction was collected in a trap maintained at 15 K. The amount of hydrogen consumed was detected by a TCD. The reduction temperature was monitored by a suitable thermocouple.

XPS spectra were recorded on an ESCA-3-MK (VG Scientific, UK) using a Mg Kα radiation source. The sample was placed in a container and was mounted on a sample probe. The sample was subjected to evacuation at 10^{-8} Torr during data collection. C1S spectra have been used as a reference with a binding energy value of 284.6 eV; the spectra of different samples were corrected for surface charging. The spectral details were computed and background subtraction was done to obtain Ni^0, Ni^{2+} and satellite peaks.

The catalysts were also examined by in situ FTIR spectra of adsorbed acetophenone. FTIR spectra (NICOLET 60SXB) were scanned in transmittance mode using self-supported wafers placed in a high temperature and high vacuum cell. The sample was activated in vacuum (10^{-6} Torr) at 673 K for 5 h, then cooled down to 373 K before recording the spectrum. Then, acetophenone was adsorbed on the sample by equilibrating at 10 mm vapour pressure for 1 h. The weakly adsorbed acetophenone was removed by evacuating the sample chamber again for a period of 1 h and the spectrum of adsorbed acetophenone was recorded.

2.3. Activity measurement

The activities of the catalysts prepared were tested for the hydrogenation of acetophenone and its derivatives in a 3×10^{-4} m^3 capacity stirred autoclave reactor made of SS 316 supplied by Parr Instrument Co., USA. It was equipped with arrangements for cooling coil, gas inlet/outlet and sampling of the liquid phase. Automatic temperature control, variable ag-

itation speed, safety rupture disc, high temperature cut-off and pressure recording by a transducer were also provided. A storage reservoir for H$_2$ gas was used along with a constant pressure regulator for supply of H$_2$. This allowed the determination of H$_2$ consumption as a function of time, while maintaining the reactor at a constant desired pressure.

In a typical catalyst recycle experiment, after completion of the first reaction, the contents in the reactor were cooled to room temperature. The unreacted H$_2$ was discharged from the reactor and the contents flushed with N$_2$, two to three times. A fresh charge of acetophenone was added through a dip tube of the reactor and the hydrogenation was carried out again as described above.

The analysis of liquid samples for the quantitative estimation of the substrate consumed and reaction products was carried out using HP 5480 gas chromatograph. A column packed with 10% OV 17 on Chromosorb W with 5 m length was used. The other conditions of analysis were oven temperature: 423 K; injection temperature: 473 K; FID temperature: 523 K and N$_2$ (carrier) gas flow rate: 4×10^{-5} m^3 min^{-1}.

3. Results and discussion

3.1. Monometallic catalysts

The results on the activity of several supported Ni catalysts for the hydrogenation of acetophenone are shown in Table 1. The activity of the catalysts has been explained in terms of turn over frequencies (TOFs) determined for constant reaction time. It was ensured that the results on catalyst activity obtained in the present work were under kinetically controlled conditions. For this purpose, the initial rate data were analysed to check the significance of gas–liquid, liquid–solid and intraparticle mass transfer effects following the quantitative criteria described by Ramachandran and Chaudhari [17]. According to these criteria, factors α_1, α_2 and ϕ_{exp} defined as the ratios of the observed rate of reaction to the maximum rates of gas–liquid, liquid–solid and intraparticle mass transfer rates, respectively, were calculated as follows:

$$\alpha_1 = \frac{R_A}{k_1 a_B A^*} < 0.1 \tag{1}$$

Table 1

The hydrogenation of acetophenone using different supported Ni catalysts[a]

S. No.	Catalyst	% Conversion	Product distribution (% selectivity)				TOF	L (nm)	L (nm)
			PEA	Styrene	Ether	EB		XRD	TPD
1	20% Ni/Al$_2$O$_3$	10	100	–	–	–	1.2	25	31
2	20% Ni/TiO$_2$	10	100	–	–	–	1.2	20	29
3	20% Ni/SiO$_2$	40	95	–	–	5	5.8	30	18
4	20% Ni/H-ZSM5	25	95	–	–	5	3.2	25	16
5	20% Ni/HY	75	75	5	5	15	10.7	15	20
6	10% Ni/HY	70	74	5	7	14	19.7	12	21

[a] Reaction conditions: concentration of acetophenone: 0.84 kmol m^{-3}; catalyst: 10 kg m^{-3}; hydrogen pressure, P_{H_2}: 30 atm; solvent: MeOH; temperature: 373 K; agitation speed: 15 Hz; reaction volume: 1 × 10^{-4} m^3; reaction time: 2 h. Surface area of supports: Al$_2$O$_3$: 1.5 × 10^5 m^2 kg^{-1}; SiO$_2$: 5 × 10^4 m^2 kg^{-1}; TiO$_2$: 3 × 10^4 m^2 kg^{-1}; HZSM-5: 2.5 × 10^5 m^2 kg^{-1}; HY: 5 × 10^5 m^2 kg^{-1}.

$$\alpha_2 = \frac{R_A}{k_s a_p A^*} < 0.1 \qquad (2)$$

$$\phi_{exp} = \frac{d_p}{6} \left[\frac{\rho_p R_A}{w D_e A^*} \right]^{0.5} < 0.2 \qquad (3)$$

The values of gas–liquid and liquid–solid mass transfer coefficients and diffusivity were calculated using correlations of Chaudhari et al. [18], Sano et al. [19] and Wilke and Chang [20], respectively. The tortuosity of the catalyst was assumed to be 3.5. The solubility data for H$_2$ in methanol (MeOH) was used from the work of Radhakrishnan et al. [21]. This analysis showed that the values of α_1, α_2 and ϕ_{exp} were below 0.01, 0.09 and 0.15, respectively, clearly indicating the absence of mass transfer resistances for the data at $d_p = 10^{-5}$ m. It can be seen from Table 1 that a 10% Ni-supported-on-zeolite Y catalyst offered the best activity for the hydrogenation of 1-phenyl ethanone (acetophenone). This is due to the fact that particle size of metal supported on the zeolite is smaller than that of metal supported on other supports. The products formed during the course of hydrogenation were found to be 1-phenyl ethanol (PEA), phenylethane (ethyl benzene (EB)), 1-methoxy-1-phenyl ethane (phenyl ethyl methyl ether (PEME), when MeOH was used as a solvent) along with trace amounts of phenethylene (styrene). These products were identified by GC and GC-MS, and in some cases, were separated by column chromatographic technique, purified and analysed. The overall material balance of the reactants (H$_2$ and acetophenone) consumed and products formed was found to be >90%. A typical concentration–time profile for the hydrogenation of

acetophenone at 393 K is shown in Fig. 1a, in which only the product PEA is shown. For the hydrogenation of 1-(4-hydroxyphenyl) ethanone (p-hydroxy acetophenone) and 4-(propyl-2-methyl)-1-phenyl ethanone (p-isobutyl acetophenone), it was observed that the reaction pathway was similar to that of hydrogenation of acetophenone from the product analysis using GC and GC-MS. Hence, a generalised reaction scheme was proposed for the hydrogenation of acetophenone, p-hydroxy acetophenone and p-isobutyl acetophenone, as shown in Scheme 1.

The typical concentration–time profiles for the hydrogenation of p-hydroxy acetophenone and p-isobutyl acetophenone at 393 K using a 10% Ni-supported-on-zeolite Y catalyst are shown in Fig. 1b and c. It was observed that the amount of styrene derivative formed was less than 5% for all the three substrates under investigation and hence, was not shown in the concentration–time profiles; however, it has been included in the reaction scheme. The major products formed during hydrogenation of 1-(4-hydroxyphenyl) ethanone (p-hydroxy acetophenone (p-HAP)) were 1-(4-hydroxyphenyl) ethanol (p-hydroxyphenyl ethanol (p-HPE)), 1-(4-hydroxy-phenyl), 1-methoxy-ethane (p-hydroxyphenyl ethyl methyl ether (p-HPEME)) and 1-(4-hydroxyphenyl) ethane (p-hydroxy ethyl benzene (p-HEB)). Correspondingly, the different products formed during hydrogenation of 4-(propyl-2-methyl), 1-phenyl ethanone (p-isobutyl acetophenone) were found to be 1-(4-hydroxyphenyl) ethanol (p-isobutyl phenyl ethanol (p-IBPE)), 1-(4-isobutylphenyl), 1-methoxy ethane (p-isobutyl phenyl ethyl methyl ether (p-IBEther)) and 4-(propyl-2-methyl), 1-phenyl
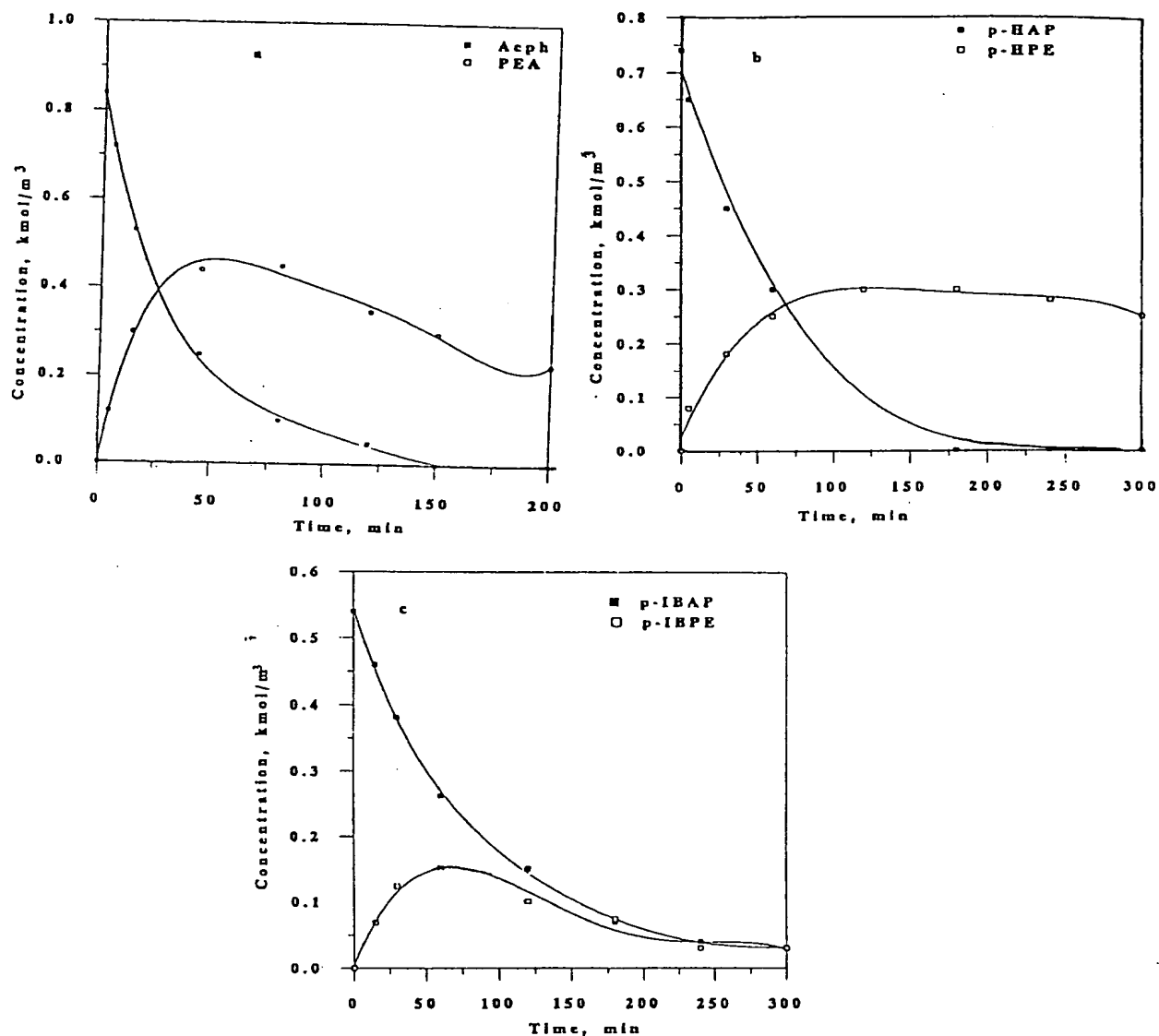
Fig. 1. Concentration–time profile for (a) the hydrogenation of acetophenone, (b) the hydrogenation of p-hydroxy acetophenone, (c) the hydrogenation of p-isobutyl acetophenone using 10% Ni/HY catalyst at 393 K.

ethane (p-isobutyl ethyl benzene (p-IBEB)). It was observed that, at higher partial pressures of hydrogen and at longer reaction times, further hydrogenolysis of the ether derivative occurred, leading to the formation of the EB derivative; this reaction step has been considered in the reaction in Scheme 1. The hydrogenolysis of p-isobutyl phenyl ethyl methyl

ether to p-isobutyl ethyl benzene has been reported by Rajashekharam and Chaudhari [22] using a 10% Ni-supported-on-zeolite Y catalyst.

3.1.1. XRD and TPD

The X-ray line broadening analysis was performed for these monometallic catalysts and the results are
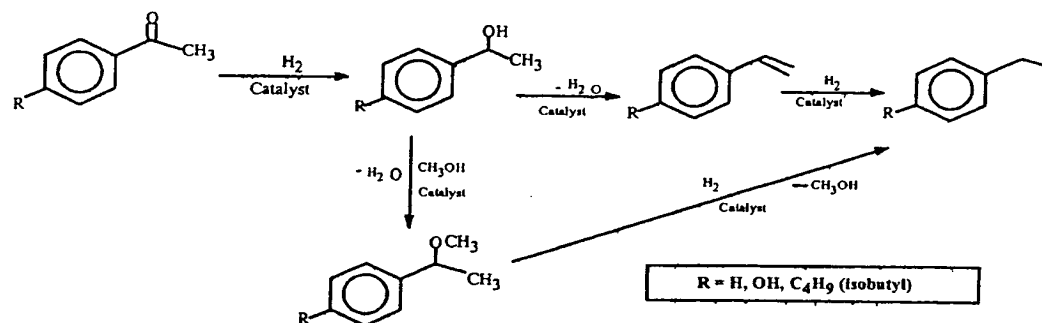
Scheme 1. Reaction scheme for the hydrogenation of substituted acetophenone derivatives using Ni and bimetallic Ni–Pt supported on zeolite Y catalysts.

presented in Table 1. For a 10% Ni-supported-on-zeolite Y catalyst, the average metal particle size was found to be ~12 nm. These average Ni particle sizes were calculated with the Sherrer equation by analysis of the Ni (1 1 1) peak at $2\theta = 44.3°$ (see Fig. 5). Table 1 also includes the values of Ni dispersion and crystallite sizes from the TPD of H_2. TPD spectra for monometallic catalysts are shown in Fig. 2. The
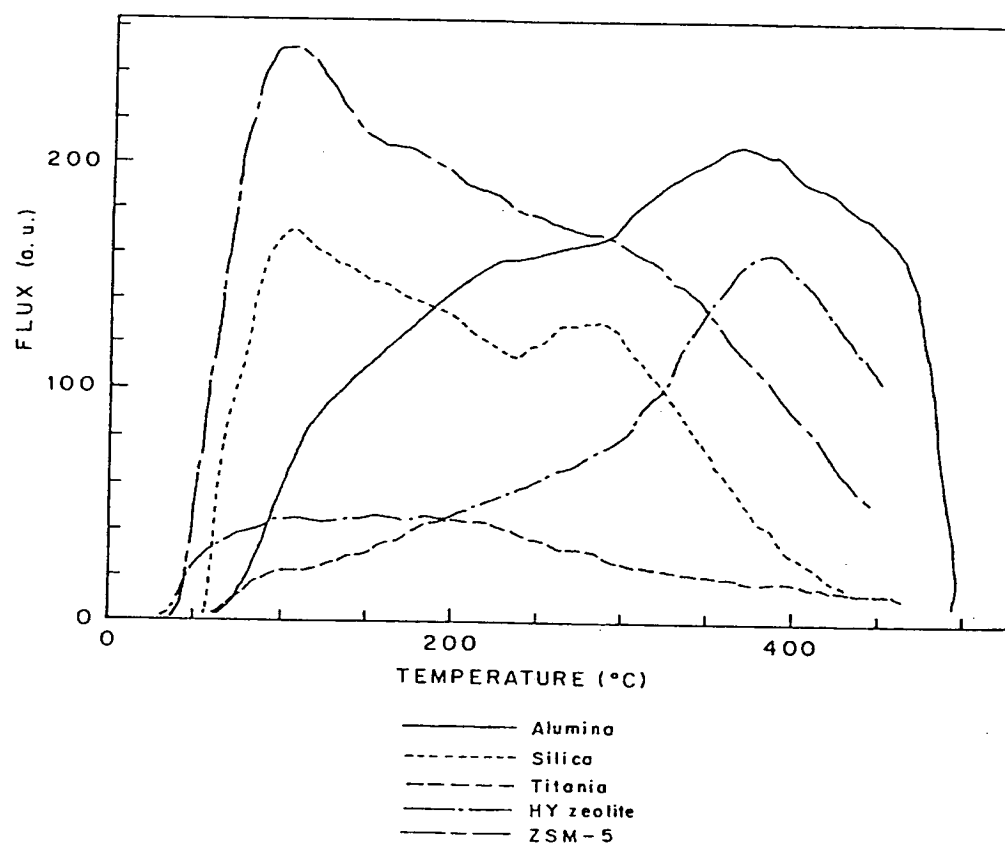

Fig. 2. TPD of 20% Ni on various supports.

degree of Ni dispersion was evaluated assuming that the ratio of the total amount of adsorbed hydrogen atom to exposed Ni atom is 1 : 1. It was observed that, among the oxide supported Ni catalysts, Ni/SiO$_2$ showed the highest hydrogen adsorption and this was directly proportional to its catalytic activity. It is interesting to note that, for 20% Ni-supported-on-HZSM-5 catalyst, the metal dispersion is highest among the 20% Ni supported catalysts even though the activity is lower than that of 20% Ni/SiO$_2$ catalyst. Similar observations were reported by Rode et al. [23] for the hydrogenation of nitriles in which the changes in the catalytic activity was attributed to different surface geometry of the nickel particles. It was also observed that the particle size decreased with increase in the metal dispersion, possibly due to the increase in exposed Ni atoms on the surface. However, the metal particle sizes calculated from TPD measurements do not match very well with the particle sizes calculated from the line broadening analysis of XRD even though the trend of decreasing particle size remains the same, as observed from the calculations made using both the techniques. TEM of monometallic Ni/zeolite Y indicated that segregates of Ni particles of different sizes and shapes are formed, leading to a lower degree of dispersion and highly disordered nature of the catalyst.

3.1.2. TPR

TPR spectra for monometallic catalysts showed a single peak in the range of 740–773 K for all samples, indicating reduction of Ni^{2+} to Ni^0 [24]. However, the hydrogen consumption varied from 73 to 95%, for various catalysts and was maximum for Ni-supported-on-zeolite Y catalyst. This is in agreement with the activity results showing the conversion of acetophenone to be higher for Ni-supported-on-zeolite Y catalysts than that for other catalysts (see Table 1).

3.1.3. XPS

The XPS spectra of both Ni and bimetallic Ni–Pt catalysts are shown in Fig. 3. For monometallic Ni supported catalyst (Fig. 3b), three peaks corresponding to Ni^0, Ni^{2+} and Ni$_{sat}^{2+}$ were observed, consistent with the reported literature for Ni-supported catalysts [25,26]. The predominant peak of Ni^{2+} in monometal-
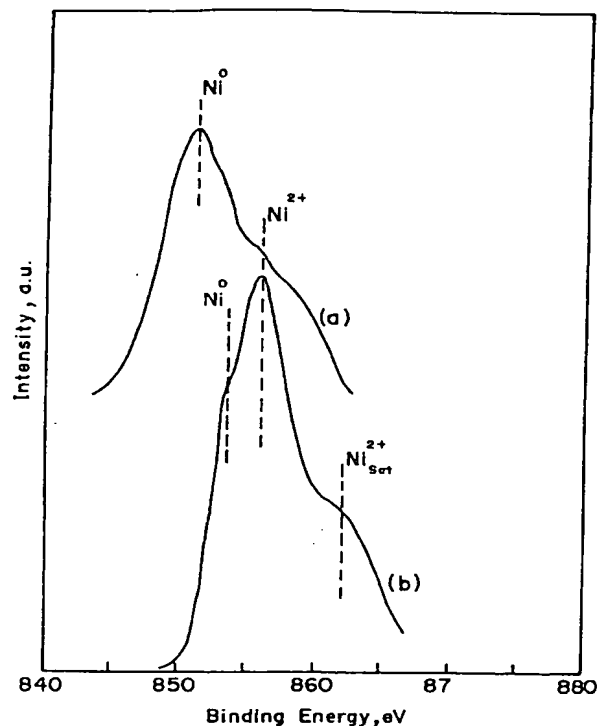

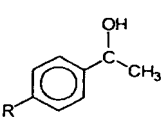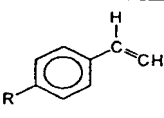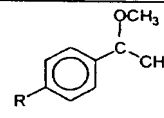Fig. 3. XPS spectra of 10% Ni–1% Pt/HY (a) and 10% Ni/HY (b).
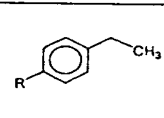
lic Ni catalysts clearly indicates the incomplete reduction of Ni^{2+} in monometallic Ni catalysts.

3.1.4. Role of solvents

The effect of solvents on the activity and selectivity of 10% Ni/zeolite Y catalyst was investigated at 373 K and 30 atm pressure of hydrogen. The results are presented in Table 2. It has been found that polar protic solvents yield better rates than aprotic solvents. The formation of ether derivatives was observed in case of MeOH, ethanol (EtOH) and isopropanol solvents, due to the solvent interactions with the resonance-stabilised carbocation of secondary alcohol derivatives. This type of solvent interactions during liquid phase hydrogenation has been reported earlier [27,28]. Another important observation was that the formation of the corresponding ether product increases as the substituent group changes (acetophenone < p-hydroxy acetophenone < p-isobutyl acetophenone). This trend was found to be similar for all the solvents investigated. Among these substituents,

Table 2

The hydrogenation of acetophenone and its derivatives: role of solvents[a]

S. No.	Solvent	% Conversion	Product distribution (% selectivity)				TOF	Dielectric constant (ε)
			(iv)	(v)	(vi)	(vii)		
1	MeOH	70	74	5	7	14	19.7	32.6
		62	70	4	13	13	15.6	
		57	65	4	20	11	10.0	
2	EtOH	75	70	4	5	21	22.4	24.6
		68	71	4	15	10	16.2	
		60	68	4	19	9	10.4	
3	iso-PrOH	85	60	4	31	5	22.1	18.3
		62	58	4	28	10	14.8	
		73	45	3	43	9	12.6	
4	n-Hexane	10	100	–	–	–	2.4	1.9
		10	95	–	–	5	2.2	
		8	90	–	–	10	1.3	

[a] From columns (iii) to (viii) for the first row, R = H, for the second row, R = OH and for the third row, R = C$_4$H$_9$ (isobutyl) for each catalyst. Reaction conditions: concentration of acetophenone [p-hydroxy acetophenone, p-isobutyl acetophenone]: 0.84 kmol m^{-3} [0.74 kmol m^{-3}; 0.54 kmol m^{-3}]; catalyst: 10 kg m^{-3} (10% Ni/HY); hydrogen pressure, P_{H_2}: 30 atm; temperature: 373 K; agitation speed: 15 Hz; reaction volume: 1 × 10^{-4} m^3; reaction time: 2 h.

–OH group is a strong electron donor, which can sta-bilise the carbocation formed, leading to the formation of the ether derivative. However, the ether formation was maximum for p-isobutyl acetophenone substrate, indicating that other factors such as hydrogen bonding also play an important role in such reactions.
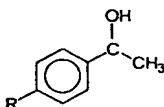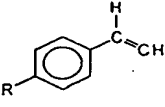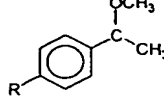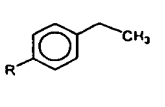
3.2. Bimetallic Ni–Pt catalysts

The results on the hydrogenation of acetophenone and its derivatives using bimetallic Ni–Pt-supported-on-zeolite Y catalysts along with the catalyst char-acterisation results on average metal crystallite size are shown in Table 3. The typical concentration–time profiles for the hydrogenation of acetophenone, p-hydroxy acetophenone and p-isobutyl acetophe-none at 373 K, using a 10% Ni–1% Pt-supported-on-zeolite Y catalyst, are shown in Fig. 4a–c. The results on the recycle study of Ni and bimetallic Ni–Pt-supported-on-zeolite Y catalysts are shown in Table 4. It was observed that the bimetallic Ni–Pt

catalysts are stable and showed constant activity on recycles. The monometallic Ni-supported-on-zeolite Y catalyst was unstable on recycle, as the catalytic activity reduced by more than 40% for all the three substrates under investigation at the first recycle it-self. These results indicate that there is a strong synergistic effect of Pt in Ni–Pt bimetallic catalysts. The effect of Pt content on the performance of the bimetallic Ni–Pt catalysts for the hydrogenation of acetophenone along with the recycle study is also shown in Tables 3 and 4. The activity increased only marginally with increase in the Pt content. This is due to increase in Pt content leading to the agglomeration of surface active Ni–Pt species and the formation of independent Pt particles in greater numbers. How-ever, all bimetallic Ni–Pt catalysts were found to be more stable and more active for at least three recycles when compared to the monometallic Ni catalysts. The presence of Pt in bimetallic Ni–Pt catalysts catalyses the reduction of Ni^{2+} to Ni^0 due to a strong syn-ergistic effect [29]. The XRD patterns of 10% Ni- and bimetallic Ni–Pt-supported-on-zeolite Y catalysts

Table 3
The hydrogenation of acetophenone and its derivatives using Ni–Pt bimetallic catalysts[a]

S. No.	Solvent	% Conversion	Product distribution (% selectivity)				TOF	L (nm)	L (nm)
			(iv)	(v)	(vi)	(vii)		XRD	TPD
1	10% Ni/HY	70	74	5	7	14	19.7	12	21
		62	70	4	13	13	15.6		
		57	65	4	20	11	10.0		
2	10% Ni–0.5% Pt/HY	81	70	2	6	22	24.4	10	20
		73	68	3	14	15	18.2		
		65	64	5	17	14	11.7		
3	10% Ni–1% Pt/HY	95	60	–	10	30	30.5	10	21
		79	70	2	10	18	21.1		
		65	61	3	16	20	12.3		
4	10% Ni–1.5% Pt/HY	95	65	2	5	28	30.0	12	20
		82	65	4	8	23	21.9		
		75	60	3	12	25	16.7		
5	10% Ni–2% Pt/HY	100	67	–	7	26	31.1	12	21
		89	58	–	10	32	25.5		
		86	60	2	18	20	16.4		
6	1% Pt/HY	5	60	3	21	16	4.75	–	–
		5	75	–	18	7	1.2		
		4	77	–	25	8	1.0		

[a] From columns (iii) to (viii) for the first row, R = H, for the second row, R = OH and for the third row, R = C_4H_9 (isobutyl) for each catalyst. Reaction conditions: concentration of acetophenone [p-hydroxy acetophenone, p-isobutyl acetophenone]: 0.84 kmol m^{-3} [0.74 kmol m^{-3}; 0.54 kmol m^{-3}]; catalyst: 10 kg m^{-3}; hydrogen pressure, P_{H_2}: 30 atm; solvent: MeOH; temperature: 373 K; agitation speed: 15 Hz; reaction volume: 1×10^{-4} m^3; reaction time: 2 h.

with varying Pt content are shown in Fig. 5. The XRD reflections indicate indirectly a synergistic effect of Pt in bimetallic Ni–Pt catalysts. The addition of Pt has definitely changed the morphology and the crystalline nature of the Ni present in the sample, as evidenced from Fig. 5. Also, the intensity of the peaks was reduced when compared to the pure Ni-supported catalyst, indicating the well-dispersed nature of the bimetallic catalysts. These reflections indicate that the addition of Pt to Ni surface would have enabled Ni to form much smaller particles that are alloyed with Pt. This is also supported by the observation that only Pt-supported-on-zeolite Y catalyst shows not only poor activity but is also unstable on recycle for all the three substrates investigated (see Tables 3 and 4).

3.2.1. TPR

Fig. 6 shows the TPR spectra for the bimetallic Ni–Pt catalysts supported on HY zeolite. In these profiles, two peaks were observed: one at about 563 K, corresponding to monometallic Pt catalyst [30] and the other at about 688 K. The second peak corresponds to that for Ni reduction, but the temperature has shifted to a lower value than that required for the monometallic Ni catalyst. This shift in the temperature of the TPR profiles has been observed earlier for Ni–Pt/SiO$_2$ catalysts, and more recently, for Ni–Pt-supported-on-modernite catalysts [31,32]. Also, the TPR profile of a physical mixture of Ni and Pt when reduced separately indicated no significant change in the temperature of reduction when compared to the Ni catalyst alone [32]. These obser-
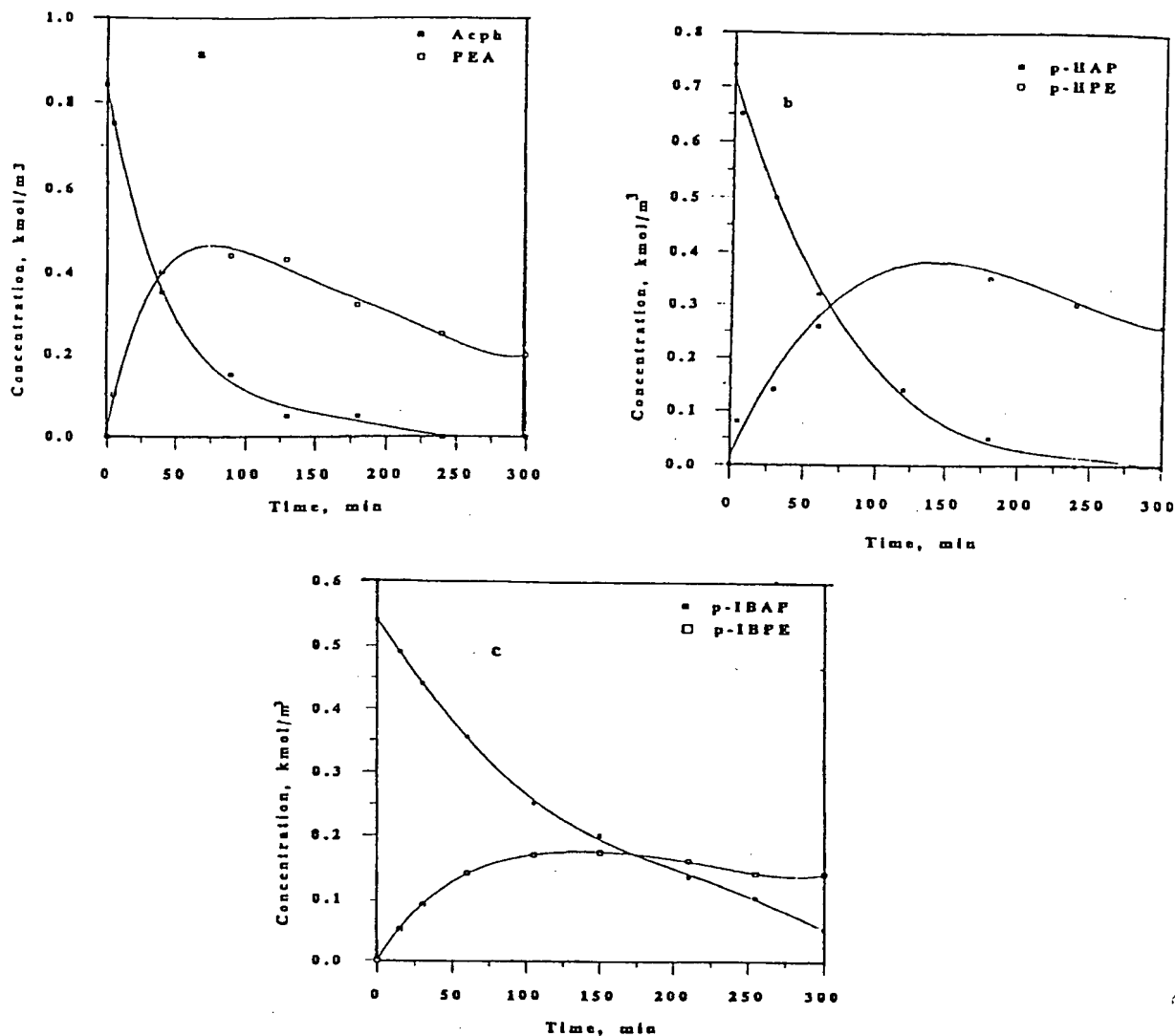
Fig. 4. Concentration–time profile for (a) the hydrogenation of acetophenone, (b) the hydrogenation of p-hydroxy acetophenone (c) the hydrogenation of p-isobutyl acetophenone using 10% Ni–1% Pt/HY catalyst at 373 K.

vations can be interpreted either as the reduction of Ni catalysed by Pt or the interaction of two metals leading to an alloy formation.

3.2.2. TEM

Transmission electron micrographs of the bimetallic Ni–Pt supported on zeolite Y catalysts showed uniform particles, close to spherical morphology. These results on TEM analysis support our XRD data, which

indicated better dispersion of Ni in bimetallic Ni–Pt catalysts. Under the present conditions of the preparation of bimetallic Ni–Pt catalysts, it is expected that a complete reduction of Ni takes place, leading to stable and uniform spherical particles.

3.2.3. XPS

The spectra of bimetallic 10% Ni–1% Pt-supported-on-zeolite Y catalyst (Fig. 3a) shows predominantly

Table 4

The hydrogenation of acetophenone and its substituted derivatives: effect of recycle study[a]

S. No.	Catalyst	TOF for different substrates		
		Acetophenone	p-HAP	p-IBAP
1	10% Ni/HY (fresh)	19.7	15.6	10.0
	Recycle 1	13.8	9.4	5.2
	Recycle 2	5.1	4.9	2.0
	Recycle 3	3.3	–	–
2	10% Ni–1% Pt/HY (fresh)	30.5	21.1	12.3
	Recycle 1	30.0	20.5	11.7
	Recycle 2	29.1	19.1	10.5
	Recycle 3	28.7	18.5	9.6
3	10% Ni–2% Pt/HY	31.1	25.5	16.4
	Recycle 1	31.4	23.6	14.1
	Recycle 2	28.6	20.8	13.6
	Recycle 3	–	–	–
4	1% Pt/HY	4.75	1.2	1.0
	Recycle 1	2.31	–	–
	Recycle 2	–	–	–
	Recycle 3	–	–	–

[a] Reaction conditions: concentration of acetophenone [p-hydroxy acetophenone, p-isobutyl acetophenone]: $0.84 \, \text{kmol m}^{-3}$ [$0.74 \, \text{kmol m}^{-3}$; $0.54 \, \text{kmol m}^{-3}$] (in the fresh run only); catalyst: $10 \, \text{kg m}^{-3}$. Hydrogen pressure, P_{H_2}: 30 atm; solvent: MeOH; temperature: 373 K; agitation speed: 15 Hz; reaction time: 2 h.
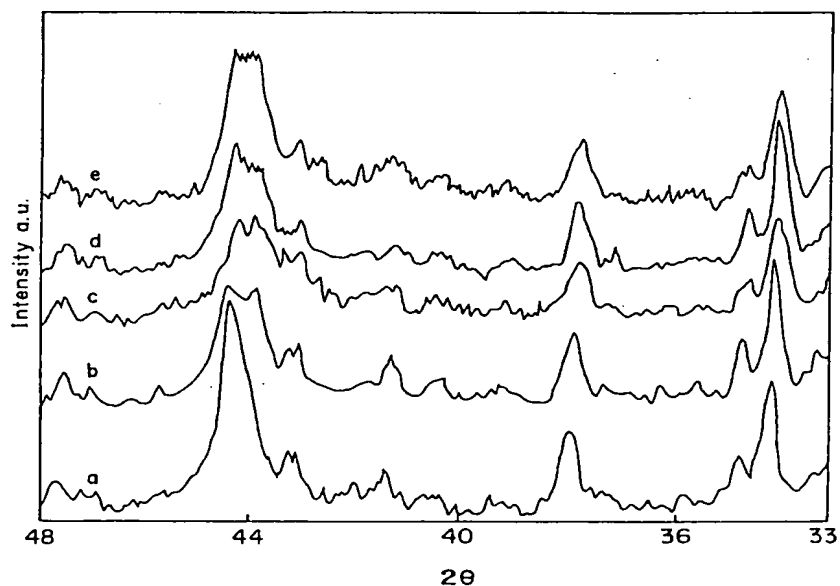

Fig. 5. XRD patterns for Ni and bimetallic Ni–Pt catalysts. a: 10% Ni/HY; b: 10% Ni–0.5% Pt/HY; c: 10% Ni–10% Ni–1% Pt/HY; d: 10% Ni–1.5% Pt/HY; e: 10% Ni–2% Pt/HY.
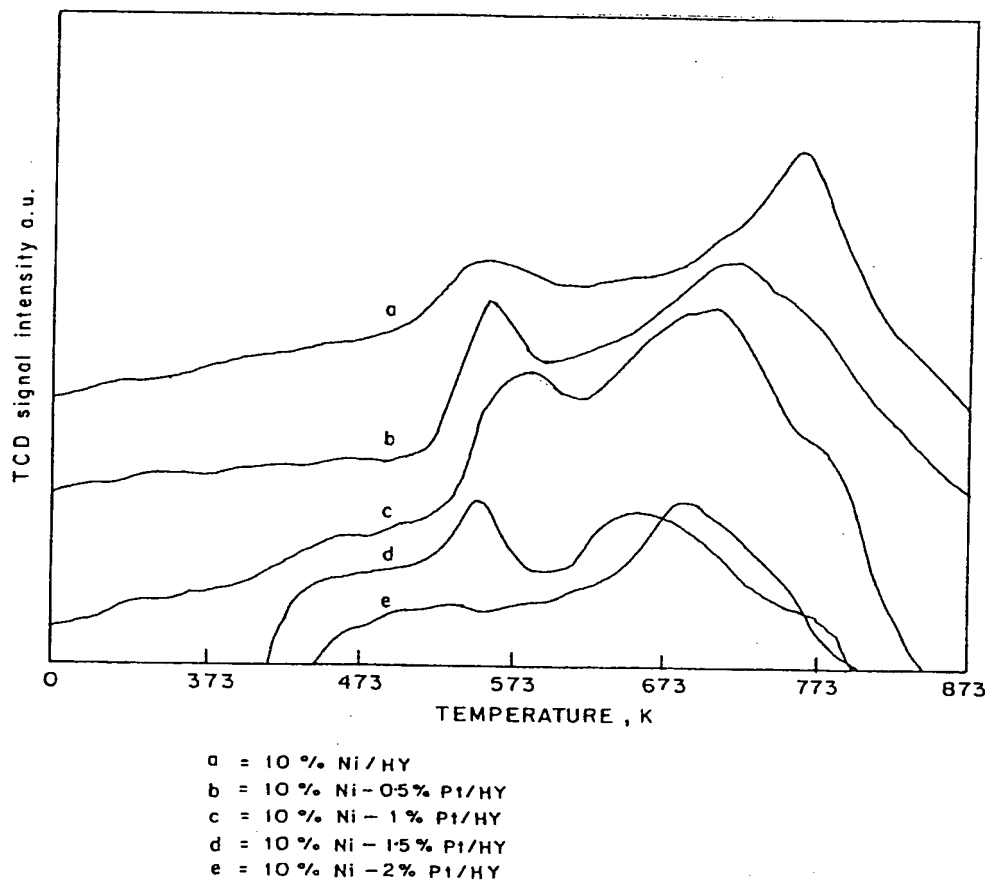
a = 10 % Ni / HY
b = 10 % Ni - 0·5% Pt / HY
c = 10 % Ni - 1 % Pt / HY
d = 10 % Ni - 1·5 % Pt / HY
e = 10 % Ni - 2% Pt / HY

Fig. 6. TPR profiles of Ni and bimetallic Ni–Pt supported on zeolite Y catalysts.

Table 5
The hydrogenation of acetophenone and its substituted derivatives: effect of promoters[a]

S. No.	Catalyst	Promoter (concentration of NaOH) (kmol m^{-3})	Substrate					
			Acetophenone		p-HAP		p-IBAP	
			% Conversion	% Selectivity PEA	% Conversion	% Selectivity p-HPE	% Conversion	% Selectivity p-IBPE
1	10% Ni/HY	0	70	74	62	70	57	65
		0.025	62	99	55	96	50	95
		0.125	60	99	53	97	50	98
2	10% Ni–1% Pt/HY	0	95	60	82	65	75	60
		0.025	86	99	73	95	67	90
		0.125	72	95	66	93	58	95

[a] Reaction conditions: concentration of acetophenone [p-hydroxy acetophenone, p-isobutyl acetophenone]: 0.84 kmol m^{-3} [0.74 kmol m^{-3}; 0.54 kmol m^{-3}]; catalyst: 10 kg m^{-3}; hydrogen pressure, P_{H_2}: 30 atm; solvent: MeOH; temperature: 373 K; agitation speed: 15 Hz; reaction volume: 1×10^{-4} m^3; reaction time: 2 h.

the existence of Ni^0 in the sample. For the bimetallic Ni–Pt catalyst, the binding energy of the Ni $2_{p3/2}$ line (Ni^0) is significantly lower (851 eV) than that of corresponding line for the monometallic Ni catalyst. This lowering in binding energy for Ni–Pt catalysts clearly indicates that, in bimetallic catalysts, Ni is completely in the reduced form (Ni^0). Also, the absence of peaks corresponding to Ni^{2+} in bimetallic catalysts indicates that the addition of Pt catalysed the reduction of Ni^{2+} to Ni^0, which is responsible for the hydrogenation reaction. These observations are consistent with the observation that the activity of recycled bimetallic Ni–Pt catalysts was the same as that of the fresh one.

3.3. Role of promoters

The roles of different organic and inorganic bases as promoters in improving the selectivity towards the secondary alcohol derivatives were investigated. The results in Table 5 indicate that NaOH plays an important role in improving the selectivity, while organic bases such as pyridine and piperidine inhibit the reaction. Also, for both Ni and bimetallic Ni–Pt catalysts, the role of NaOH is significant in improving the selectivity. In most cases, selectivities >95% were observed when NaOH was used. In the presence of a base like NaOH, initially, an enolate ion is formed [33]. Adsorption of this species on the catalyst and hydride ion transfer from the catalyst, followed by protonation from the solution, gives almost selectively the secondary alcohol, as shown in Scheme 2. Also, the presence of a base causes neutralisation of acidic sites present on the catalyst which would otherwise cause the dehydration of the secondary alcohol already formed. This is discussed in more detail under Section 3.4.

3.4. Reaction mechanism

The difference in the activities of Ni and Ni–Pt bimetallic catalysts indicates strong interactions of the substrates under investigation with various active sites, indicating a possibility of different types of mechanisms operating for these catalysts. In Ni-supported-on-zeolite Y, the activity of the catalysts depends on the extent to which two different types of

active sites for hydrogenation are formed. The first site means the metallic Ni sites at exchanged protons of the zeolite where small Ni clusters are formed during calcination/activation [34]. The second active site, which is present in excess in pure metallic Ni form, covers the external surface area of the zeolite during the precipitation process of the catalyst and consequent steps of calcination/activation. In bimetallic Ni–Pt catalysts, the addition of Pt to Ni forms a miscible alloy of Ni–Pt fostering the stability of reduced Ni. In this case, the hydrogen adsorption is increased due to the presence of well-dispersed Ni–Pt particles. It has been speculated by Raab and Lercher [35] that, for gas phase hydrogenation of crotonaldehyde, the hydrogenation rate increases for Ni–Pt/SiO$_2$ due to the interactions of C=O group with the bimetallic catalyst.

Different FTIR spectra of acetophenone adsorbed at 373 K on 10% Ni-, 10% Ni–1% Pt-, 1% Pt-supported-on-zeolite Y and pure zeolite Y samples are presented in Fig. 7. In the region of hydroxyl group stretching vibrations, disappearance of peaks (−ve peaks) at 3745, 3695, 3625 and 3675 cm^{-1}, is attributed to perturbation and shifting to lower frequency due to interaction with both benzene ring and the C=O bond of adsorbed acetophenone. These −OH groups are assigned to surface silinol, extra lattice silica–alumina debris, bridging acidic OH groups situated in super cages and those in sodalite cages, respectively [36]. It can be seen that relatively fewer acidic OH groups are affected in the modified zeolite Y than on pure zeolite Y samples. In Fig. 7a–d, FTIR spectra of the acetophenone adsorbed (1800–1350 cm^{-1}) on the catalyst samples (HY zeolite, 10% Ni-supported-on-zeolite Y, bimetallic 10% Ni–1% Pt-supported-on-zeolite Y and 1% Pt-supported-on-zeolite Y samples) are presented. The characteristic C=O group vibration which occurs at 1685 cm^{-1} for pure acetophenone is shifted to 1670 cm^{-1}, due to the weakening of the C=O vibrations because of strong interactions with the protons in zeolite. The fact that the shift (15 cm^{-1}) is the same for all the samples indicates that the interaction is energetically not different for all the samples under investigation. Bosacek and Kubelkara [37] have also reported a similar type of observation. In their study, the shift was in C=O frequency in the case of acetone adsorbed on zeolite Y and HZSM-5 zeolites.

Scheme 2. .

a = H Y
b = 10 % Ni / HY
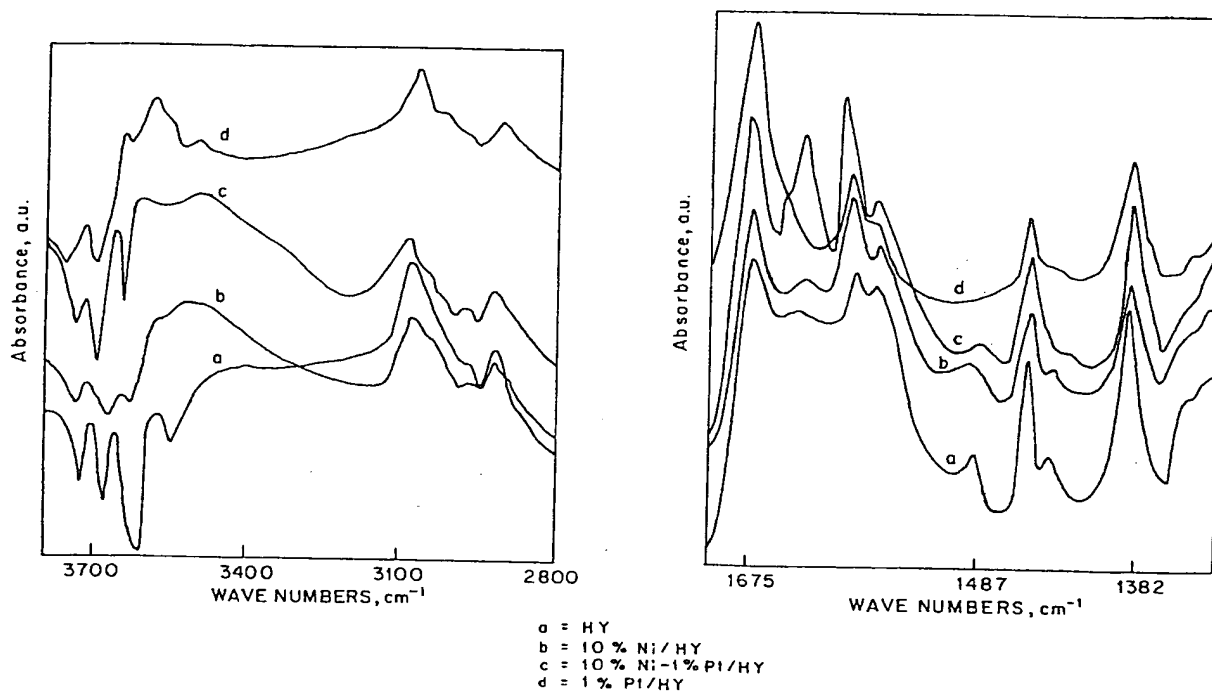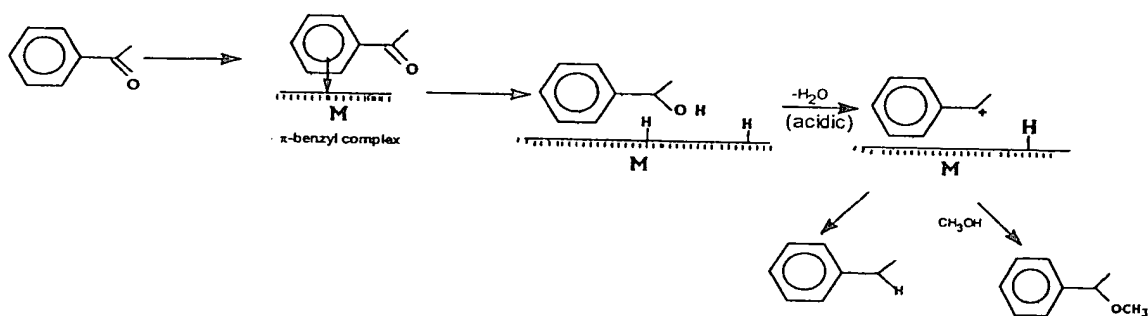c = 10 % Ni–1% Pt / HY
d = 1 % Pt / HY
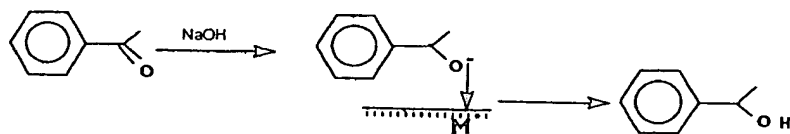
Fig. 7. FTIR spectra of acetophenone adsorbed catalysts.

Scheme 3. Schematic representation of the reaction mechanism.

Another feature in the spectra of adsorbed acetophenone is the appearance of additional bands at around $1625\,cm^{-1}$, other than pure acetophenone. This is probably due to the adsorption of reaction products of acetophenone like phenyl ethyl alcohol, as reported by Venuto and Landis [38]. Thus, the role of Pt in the bimetallic Ni–Pt catalyst is to catalyse the reduction of Ni^{2+} to Ni^{0} and it does not significantly activate the C=O bond during the catalytic process. It was speculated that the C=O bond is highly activated due to the strong interactions with the zeolitic proton [37], leading to the formation of a charge-delocalised CO bond, and hydride attack from the catalyst surface is facilitated. Also, a third type of site responsible for the ether formation is shown in Scheme 3; this is essentially the acidic site present in the zeolite support. First, the formation of a π-benzyl complex is believed to take place [39], and due to acidic sites present on the catalyst, dehydration of the secondary alcohol derivative takes place, leading to a carbocation which is resonance-stabilised. This carbocation interacts in SN1 fashion, forming ether derivatives if MeOH is used as a solvent. The presence of a base eliminates the dehydration route, giving highest selectivity to secondary alcohol.

4. Conclusions

Hydrogenation of acetophenone and its substituted derivatives was studied using Ni and bimetallic Ni–Pt on various supports. It was found that 10% Ni-supported-on-zeolite Y gave the best activity among the monometallic catalysts for the hydrogenation of acetophenone and its substituted derivatives. Bimetallic Ni–Pt catalysts were found to be more active and stable as compared to monometallic Ni catalysts. The catalyst characterisation results revealed that doping of Pt catalyses the complete reduction of Ni^{2+} to Ni^{0}, leading to the higher activity of these catalysts. FTIR studies showed that the interactions of the zeolite support with intermediates formed during the course of hydrogenation and solvent moieties (MeOH in this work) led to the formation of ether derivatives. Addition of a trace amount of base like NaOH improves tremendously the selectivity towards the secondary alcohol derivatives.

5. Notation

A	hydrogen
A^{*}	concentration of A at the gas–liquid interface $(kmol\,m^{-3})$
a_p	external surface area of the catalyst per unit volume $(m^2\,m^{-3})$
B	concentration of reactant B $(kmol\,m^{-3})$
D_e	effective diffusivity $(m^2\,s^{-1})$
d_p	diameter of catalyst particle (m)
R_A	rate of hydrogenation reaction $(kmol\,m^{-3}\,s^{-1})$
w	catalyst loading $(kg\,m^{-3})$

5.1. Greek letters

α_1	parameter defined by Eq. (1)
α_1	parameter defined by Eq. (2)
ϕ_{exp}	parameter defined by Eq. (3)
ρ_s	particle density $(kg\,m^{-3})$

Acknowledgements

References

[1] P.L. Mills, P.A. Ramachandran, R.V. Chaudhari, Chem. Eng. Rev. 8 (1992) 1.

[2] V. Elango, Eur. Patent 400,892 (Cl.C07c57/30) (1990).

[3] I Kim, Chem. Eng. December 100 (1993) 94.

[4] P.S. Kumbhar, Appl. Catal. A: Gen. 96 (1993) 241.

[5] D.L. Shawn, D.K. Sanders, M.A. Vannice, Appl. Catal. A: Gen. 113 (1994) 59.

[6] M.A. Aramendia, V. Borau, C. Jimenez, J.M. Marinas, M.E. Sempere, P. Urbano, Appl. Catal. A: Gen. 43 (1988) 41.

[7] J.H. Sinfelt, Bimetallic Catalysts-Discoveries, Concepts and Applications, Wiley, NY, USA, 1983.

[8] A. Rochefort, J. Andzelm, N. Russo, D.R. Salahub, J. Am. Chem. Soc. 112 (1990) 8239.

[9] J. Masson, S. Vidal, P. Cividino, P. Fouilloux, J. Court, Appl. Catal. A: Gen. 99 (1993) 147.

[10] S. Hamar-Thibault, J. Masson, P. Fouilloux, J. Court, Appl. Catal. A: Gen. 99 (1993) 131.

[11] M.V. Rajashekharam, R.V. Chaudhari, Catal. Lett. 41 (1996) 171.

[12] J.P. Roberts, Hydrogenation Catalysts, Noyes Data Corporation, Park Ridge, NJ, USA, 1976.

[13] S.R. Robertson, R.B. Anderson, J. Catal. 33 (1971) 286.

[14] M. Khaidar, C. Allibert, J. Driole, P. Germi, Mater. Res. Bull. 17 (1982) 329.

[15] M. Arai, K. Suzuki, Y. Nishiyama, Bull. Chem. Soc. Jpn. 66 (1993) 40.

[16] M. Arai, Y. Nishiyama, T. Masuda, K. Hashimoto, Appl. Surf. Sci. 89 (1995) 11.

[17] P.A. Ramachandran, R.V. Chaudhari, in: Three Phase Catalytic Reactors, Gordon and Breach, New York, 1983.

[18] R.V. Chaudhari, R.V. Gholap, G. Emig, H. Hofmann, Can. J. Chem. Eng. 65 (1987) 774.

[19] Y. Sano, N. Yamaguchi, T.J. Adachi, Chem. Eng. Jpn. 1 (1974) 255.

[20] C.R. Wilke, P. Chang, AIChE J. 1 (1955) 264.

[21] K. Radhakrishnan, P.A. Ramachandran, P.H. Brahme, R.V. Chaudhari, J. Chem. Eng. Data 28 (1983) 1.

[22] M.V. Rajashekharam, R.V. Chaudhari, Chem. Eng. Sci. 51 (1996) 1663.

[23] C.V. Rode, M. Arai, M. Shirai, Y. Nishiyama, Appl. Catal. A: Gen. 148 (1997) 405.

[24] N.W. Hurst, S.J. Gentry, A. Jones, B.D. McNicol, Catal. Rev. Sci. Eng. 24 (1982) 233.

[25] L. Daza, B. Pawelec, J.A. Anderson, J.L.G. Fierro, Appl. Catal. A: Gen. 87 (1992) 145.

[26] T.L. Xiang, Z.F. Mei, Z.L. Bin, React. Kinet. Catal. Lett. 57 (1996) 99.

[27] T. Takahashi, T. Kai, M. Tashiro, Can. J. Chem. Eng. 66 (1988) 433.

[28] L. Gilbert, C. Mercier, in: M. Guisnet (Ed.), Heterogeneous Catalysis in Fine Chemicals III, vol. 51, Elsevier, Amsterdam, 1993.

[29] P.S. Kumbhar, R.A. Rajadhyaksha, in: M. Guisnet, J. Barbier, J. Barroult, C. Bouchoule, D. Duperez, G. Perot, C. Montassier (Eds.), Heterogeneous Catalysis in Fine Chemicals III, Stud. Surf. Sci. Catal., vol. 251, Elsevier, Amsterdam, 1993.

[30] B.D. Mc Nicol, J. Catal. 46 (1977) 438.

[31] C.G. Raab, J.A. Lercher, J.G. Goodwin Jr., J.Z. Shyu, J. Catal. 122 (1990) 406.

[32] R.M. Jao, T.B. Lin, J.R. Chang, J. Catal. 161 (1996) 222.

[33] R.L. Augustine, in: D.D. Eley, S.H. Pine, P.B. Weisz (Eds.), Adv. Catal., vol. 69, Academic Press, London, 1976.

[34] K. Saeki, K. Shima, Jpn. Kokai Tokkyo Koho JP, 02,78,639 (Cl.C07C33/20) (1990).

[35] W.M.H. Sachtler, Erdol Erdgas Kohle 109 (10) (1993) 422.

[36] J.W. Ward, in: J. Rabo (Ed.), Zeolite Chemistry and Catalysis, vol. 171, ACS monograph, American Chemical Society, Washington, DC, USA 1976, p. 118.

[37] V. Bosacek, L. Kubelkara, Zeolites 10 (1990) 64.

[38] P.B. Venuto, P.S. Landis, J. Catal. 6 (1966) 237.

[39] S. Mitsui, S. Imaizumi, M. Hisashige, Y. Sugi, Tetrahedron 29 (1973) 4093.